Available online at www.sciencedirect.com
SCIENCE DIRECT

Journal of the European Ceramic Society 23 (2003) 1441–1448
www.elsevier.com/locate/jeurceramsoc

Thick-film resistors on zirconia substrates for possible strain gauge applications

Marko Hrovat[a,*], Darko Belavič[b], Andreja Benčan[a], Janez Holc[a]

[a]*Jožef Stefan Institute, Jamova 39, SI-1000 Ljubljana, Slovenia*
[b]*HIPOT, Trubarjeva 7, SI-8310 Šentjernej, Slovenia*

Received 30 May 2002; accepted 16 September 2002

Abstract

Thick-film resistors that were developed for firing on alumina substrates have been evaluated in terms of their compatibility with ZrO_2. The characteristics of a number of 10 kohm/sq. resistors that were fired on 96% alumina and on tetragonal zirconia substrates were investigated. Possible interactions between the resistor material and the zirconia were studied with X-ray powder-diffraction analysis, with scanning electron microscopy and with energy-dispersive X-ray analysis. Sheet resistivities, temperature coefficients of resistivity, current noise and gauge factors were measured. The results indicate that the evaluated thick-film resistors are compatible with zirconia ceramics.

Keywords: Resistors; Ruthenates; Strain gauges; Substrates; ZrO_2

1. Introduction

The change in resistance of a resistor under an applied stress is partly due to deformation, i.e. the changes in the dimensions of the resistor, and partly due to an alteration in the specific resistivity as a result of changes in the microstructure of the material.[1] The gauge factor (GF) of a resistor is defined as the ratio of the relative change in resistance ($\Delta R/R$) and the strain ($\Delta l/l$):

$$GF = (\Delta R/R)/(\Delta l/l) \quad (1)$$

Geometrical factors alone result in gauge factors of 2–2.5. Gauge factors higher than this are due to microstructural changes, i.e. changes to the specific conductivity. The GFs of thick-film resistors are mostly between 3 and 15. Due to their stability, temperature coefficients of resistivity (TCR) under 100×10^{-6}/K and relatively low cost, strain gauges realised with thick-film technology offer advantages in some applications over both metal films (low GF, low TCR, expensive) and semiconducting elements (high GF, high TCR, inexpensive).[2,3] Typically, four resistors connected in a Wheatstone bridge are used. For better sensitivity (greater change in the balance of the Wheatstone bridge), two resistors are normally under tension (an increase of resistance) and two under compression (a decrease of resistance). Within the same resistor series the GFs and the current noise indices of thick-film resistors increase with increasing sheet resistivity.[4,5] Therefore, in most cases 10 kohm/sq. resistors are used for the strain sensors as a useful compromise between sensitivity and relatively low noise and also because of their relatively low power consumption.

Thick-film resistors are printed and fired on a ceramic substrate (diaphragm), which is usually based on alumina. However, sensing elements made on partially stabilised tetragonal zirconia would have some improved characteristics as tetragonal zirconia has a higher mechanical strength and a lower modulus of elasticity than alumina.[6] Therefore, the operating range and the mechanical strength of sensors are improved. Some mechanical characteristics for 96% Al_2O_3, which is mostly used for the substrates of thick-film circuits, and for tetragonal ZrO_2 (Y-TZP–Y_2O_3 stabilised tetragonal zirconia) are summarised in Table 1.

* Corresponding author. Tel.: +386-1-477-3479; fax: +386-1-426-3126.
E-mail address: marko.hrovat@ijs.si (M. Hrovat).

0955-2219/02/$ - see front matter
PII: S0955-2219(02)00355-2

Table 1
Some characteristics of 96% Al_2O_3 and Y-TZP (tetragonal ZrO_2)

	Al_2O_3 (96%)	Y-TZP
Young's modulus E (GPa)	250–330	200
Flexural strength (MPa)	300	800–1200
Fracture toughness (MPa $m^{0.5}$)	3–3.5	6–8
Poisson's ratio	0.22	0.28
Hardness (VH) (GPa)	1600	1250
Density (g/cm^3)	3.6	6

Table 2
Conductive phase and summarised qualitative results of EDS microanalysis of elements detected in the glass phase of 10 k ohm^2 resistors[11,12a]

Resistor	Conductive phase	Main elements	Other elements
8039	Ruthenate	Si, Pb, Al	Zr
2041	RuO_2 + ruthenate	Si, Pb, Al	Mg, Zn, Ca, Ba
3414-A	Ruthenate	Si, Pb	Al, K
8241	RuO_2	Si, Pb, Al	Ca

[a] Boron oxide, which is also present in the glass phase, cannot be detected in the EDS spectra.

By replacing an Al_2O_3 ceramic membrane with a ZrO_2 membrane of the same thickness the operating range can be extended or alternatively, thinner and therefore more flexible membranes could be used, which is important for low pressure sensors. This is shown schematically in Fig. 1 for a diaphragm with free edges and with fixed edges, respectively. The deformation of Al_2O_3-based and tetragonal ZrO_2-based membranes was calculated using the following parameters: membrane radius, 20 mm; thickness, 0.635 mm; and pressure, 1.5×10^4 Pa.

Thick-film resistor materials are a complex mixture of conductive particles, glass phase and added oxide modifiers. All the constituents of the resistor material react with each other and with the ceramic substrate during firing.[7–10] The electrical characteristics of the resistors are the result of these reactions. As the thick-film resistors were developed for firing on alumina substrates, their compatibility with ZrO_2 needs to be evaluated.

In this paper the characteristics of some 10 kohm/sq. thick-film resistors, fired on alumina (see Refs. 11 and 12) and on zirconia substrates, will be compared. The tested resistors were 2041 (Du Pont), 8241 (Heraeus) and 3413-A (ESL). Electro Science Labs. The 3414 resistor series was specially formulated for high gauge factors.[13] Data for 8039 resistors, fired on ZrO_2 substrates which were published elsewhere,[14] are also included. The conductive phase in the 8039 and the 3414-A resistors is based on ruthenates, in the 2041 resistors on a mixture of RuO_2 and $Pb_2Ru_2O_{6.5}$, and in the 8241 resistors on RuO_2. Data on the conductive phase and the qualitative results of an energy-dispersive X-ray analysis (EDS) of the glass composition of the thick-film resistors are summarized in Table 2.[11,12] All glasses contain, as main elements, lead, silicon and aluminum oxides. Boron oxide, which is also present in the glass phase, cannot be detected in the EDS spectra because of the low relative boron weight fraction in the glass and the strong absorption of the boron K_α line during EDS analysis in the glass matrix.

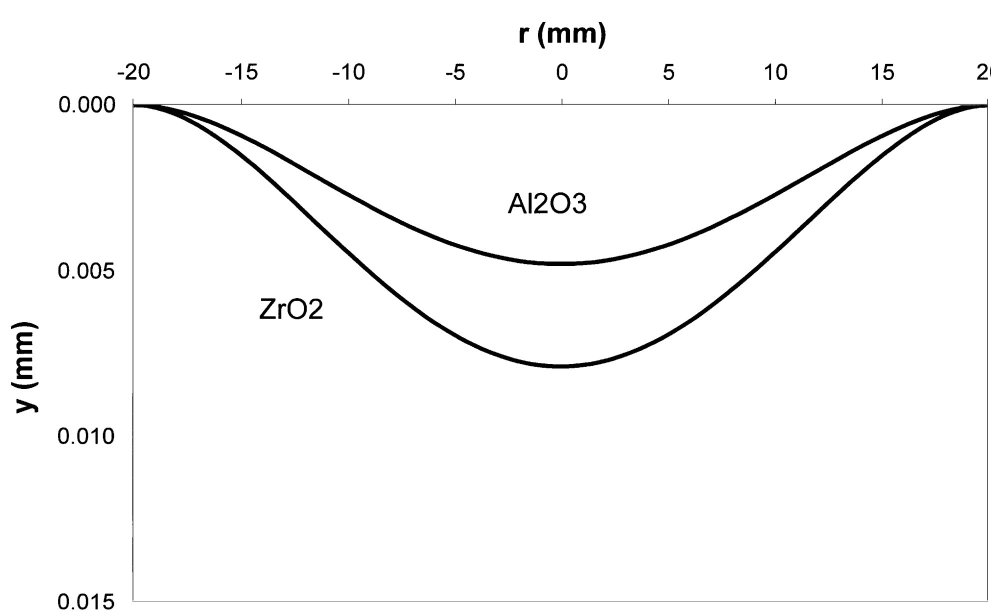

Fig. 1. The deformation of Al_2O_3-based and tetragonal ZrO_2-based ceramic membranes with fixed edges under a pressure of 1.5×10^4 Pa.

2. Experimental

Thick-film resistors, terminated with a prefired Pd/Ag conductor, were printed and fired at 850 °C for 10 min on 96% alumina and on tetragonal ZrO_2 (Y-TZP) substrates. The zirconia substrates were obtained from CoorsTek, CO, USA. For the electrical measurements the resistors (1×1 mm^2) were terminated with a prefired Pd/Ag conductor. The dimensions of the resistors for microstructural analysis and X-ray diffraction (XRD) analysis, which were printed and fired without conductor terminations, were 12.5×12.5 mm^2.

Cold (from −25 to 25 °C) and hot (from 25 to 125 °C) TCRs were calculated from resistivity measurements at −25, 25, and 125 °C. The current noise was measured in dB on 100 mW loaded resistors using the Quan Tech method (Quan Tech Model 315-C).

The changes in resistivity as a function of substrate deformation were measured with the simple device described in Ref. 15. The ceramic substrate with a printed-and-fired thick-film resistor in the middle of the substrate was supported on both sides. The load was applied to the middle of the substrate with a micrometer, which induced a tensile strain in the resistor. The magnitude of the strain is given by Eqs. (2) and (3),[16] where "d" is the deflection (m), t is the substrate thickness (m), X is the distance from the supported edge of the substrate (m) and L is the distance between the support edges (m).

$$\varepsilon = \Delta l/l = (d^* t^* X^* 12)/L^3 \qquad (2)$$

For $X = L/2$, i.e. in the middle of the substrate, where the strain is greatest, the equation transforms into:

$$\varepsilon = \Delta l/l = (d^* t^* 6)/L^2 \qquad (3)$$

The gauge factors are calculated using Eqs. (1) and (3) from the resistivity changes and the strain.

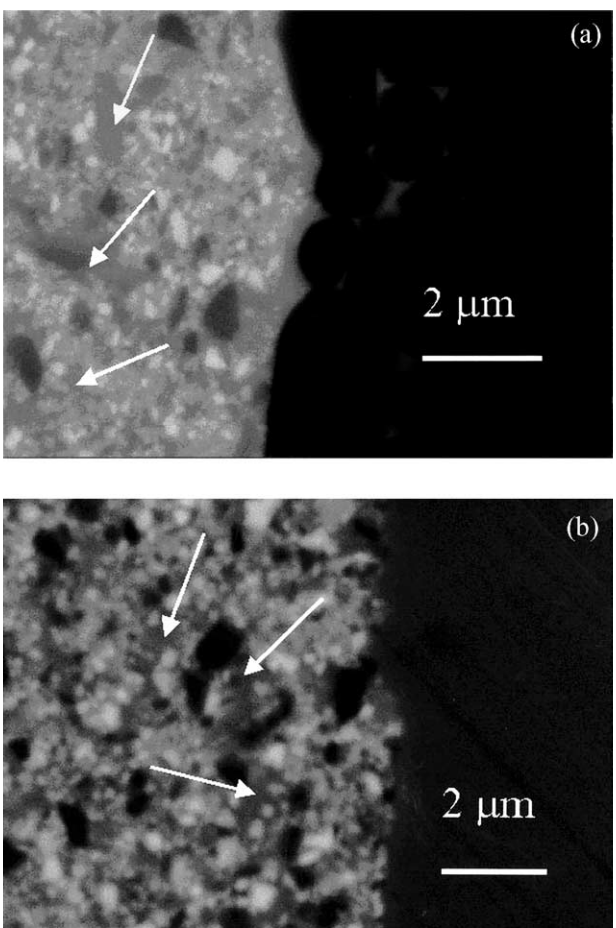

Fig. 2. (a) Microstructure of a cross-section of the 8039 thick-film resistor, fired at 850 °C on alumina. The substrate is on the right. Glass phase is indicated by arrows. (b) Microstructure of a cross-section of the 8039 thick-film resistor, fired at 850 °C on zirconia. The substrate is on the right. Glass phase is indicated by arrows.

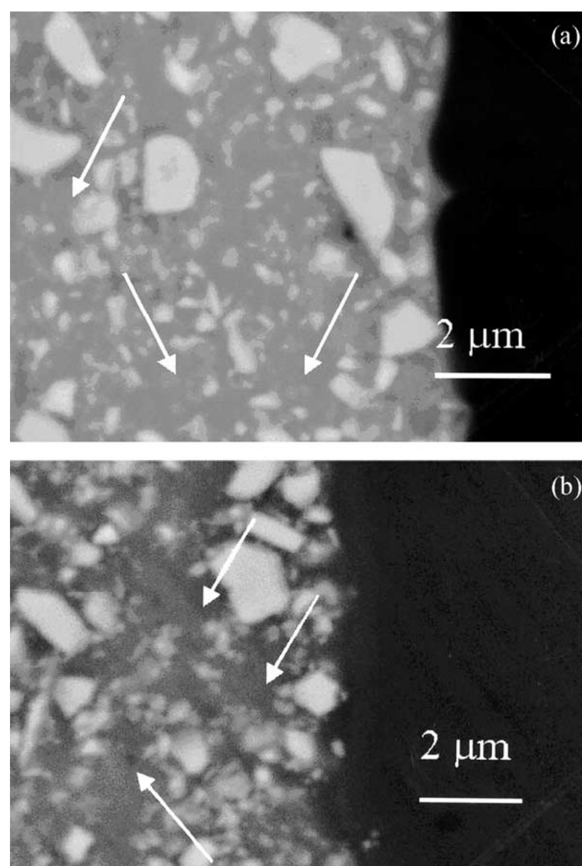

Fig. 3. (a) Microstructure of a cross-section of the 3414-A thick-film resistor, fired at 850 °C on alumina. The substrate is on the right. Glass phase is indicated by arrows. (b) Microstructure of a cross-section of the 3414-A thick-film resistor, fired at 850 °C on zirconia. The substrate is on the right. Glass phase is indicated by arrows.

For the microstructural investigation the resistors, which were printed and fired on alumina ceramics, were mounted in epoxy in a cross-sectional orientation and then cut and polished using standard metallographic techniques. A JEOL JSM 5800 scanning electron microscope (SEM) was used for the microstructural analysis. Prior to analysis in the SEM, the samples were coated with carbon to provide electrical conductivity and to avoid charging effects. The resistors, that were fired on alumina and zirconia substrates were analysed by X-ray powder diffraction (XRD) analysis with a Philips PW 1710 X-ray diffractometer using Cu K_α radiation. X-ray spectra were measured from $2\Theta=20°$ to $2\Theta=70°$ in steps of 0.04°.

3. Results and discussion

At the interface between ZrO_2 and the resistor no interactions or evidence for new phases could be detected by SEM and EDX. These results indicate the compatibility of the resistor material and the ZrO_2. The examples of microstructures of the cross-sections of

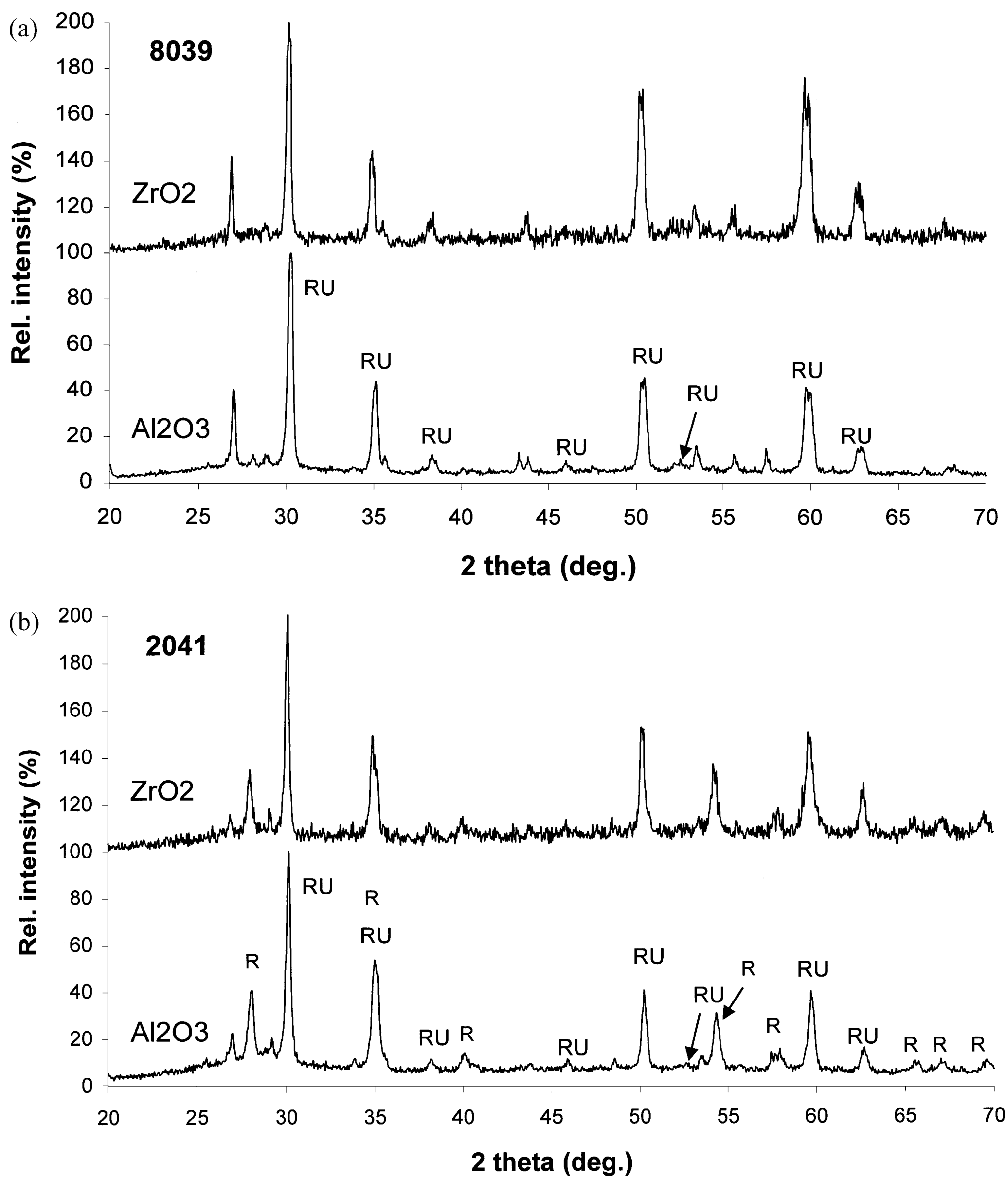

Fig. 4. (a) X-ray spectra of 8039 resistors, fired on Al_2O_3 and ZrO_2 substrates. Peaks of ruthenate phase are denoted "RU". (b) X-ray spectra of 2041 resistors, fired on Al_2O_3 and ZrO_2 substrates. Peaks of RuO_2 and ruthenate phase are denoted "R" and "RU", respectively. (c) X-ray spectra of 3414-A resistors, fired on Al_2O_3 and ZrO_2 substrates. Peaks of ruthenate phase are denoted "RU". (d) X-ray spectra of 8241 resistors, fired on Al_2O_3 and ZrO_2 substrates. Peaks of RuO_2 are denoted "R".

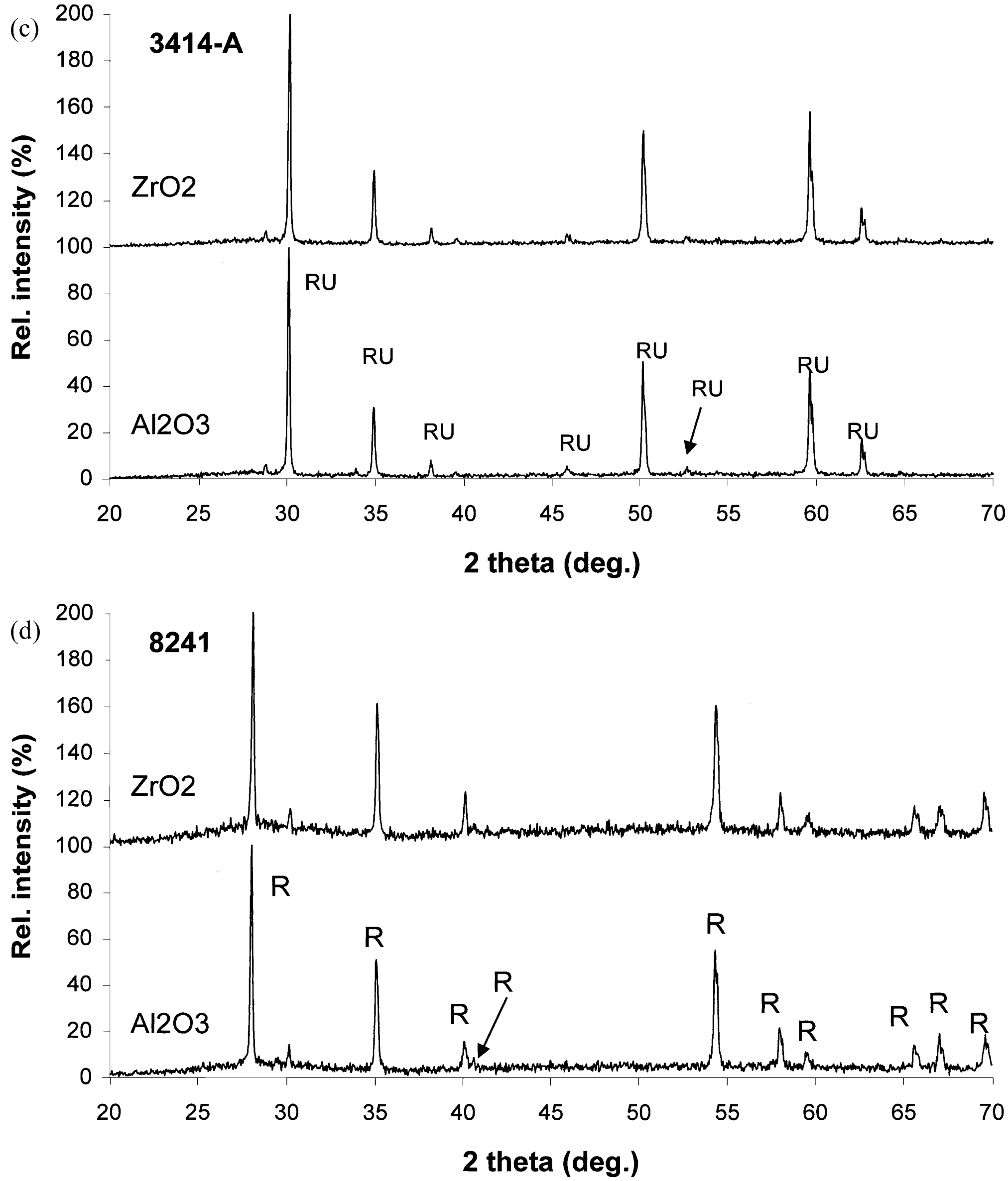

Fig. 4. (*continued*)

Table 3
Sheet resistivities, cold (−25 to 25 °C) and hot (25 to 125 °C) TCRs, noise indices and gauge factors (GFs) of the 10 k ohm^2. resistors fired on the Al_2O_3 and ZrO_2 substrates

Resistor	Substrate	R (k ohm^2)	Cold TCR ($\times 10^{-6}$/K)	Hot TCR ($\times 10^{-6}$/K)	Noise (dB)	GF
8039	Al_2O_3	7.15	50	95	−14.6	11
	ZrO_2	9.20	115	150	−13.8	10
2041	Al_2O_3	6.70	−35	20	−23.4	11
	ZrO_2	5.75	105	150	−21.6	10
3414-A	Al_2O_3	6.70	−60	5	8.2	21
	ZrO_2	11.2	40	105	0.55	16
8241	Al_2O_3	5.45	25	65	−6.0	15
	ZrO_2	1.44	245	275	−9.2	13

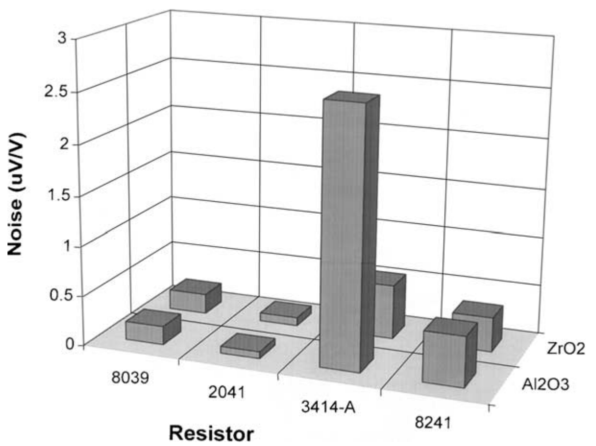

Fig. 5. Noise indices of resistors, fired on the Al_2O_3 and ZrO_2 substrates.

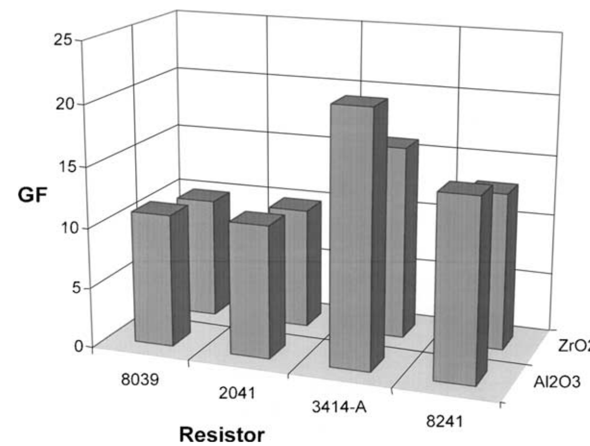

Fig. 6. Gauge factors of resistors, fired on the Al_2O_3 and ZrO_2 substrates.

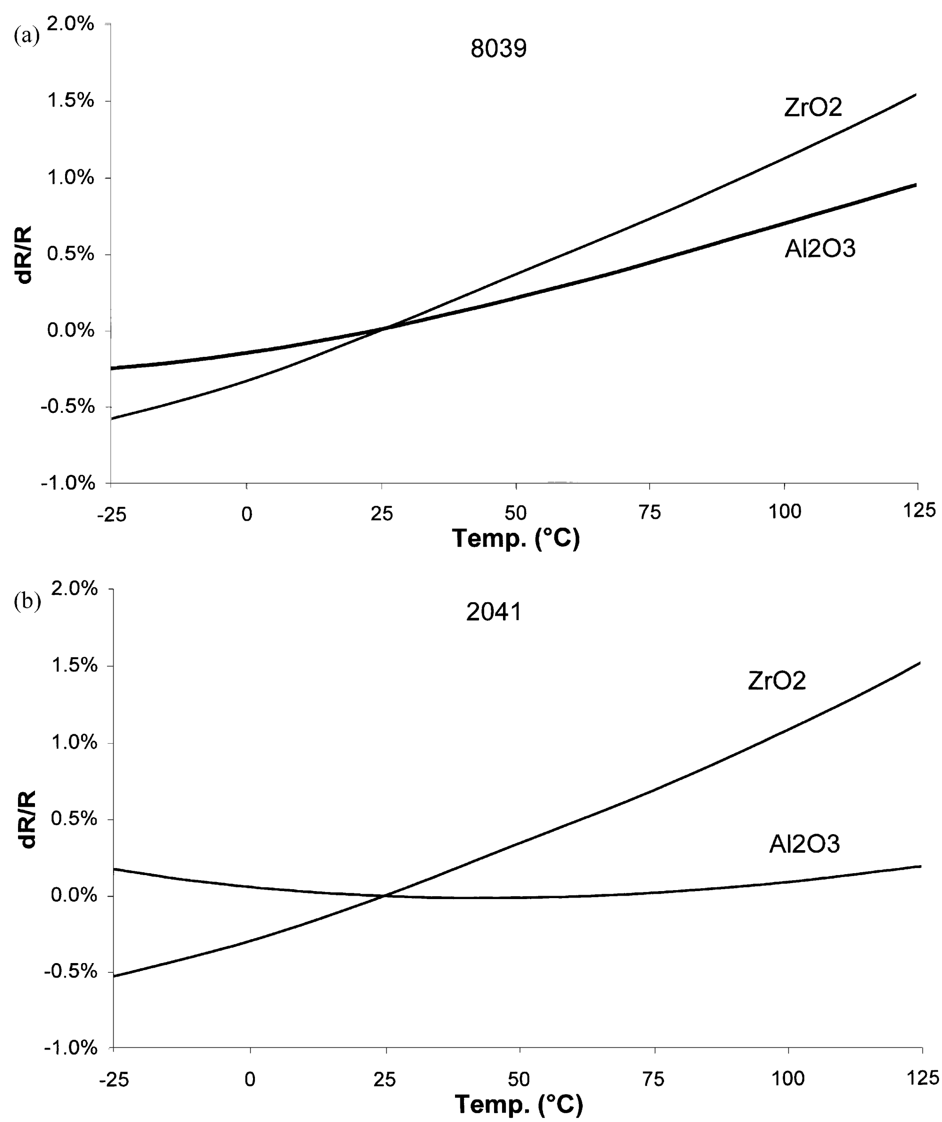

Fig. 7. (a) The dependence of relative resistivity on temperature for 8039, fired at 850 °C on Al_2O_3 and ZrO_2 substrates. (b) The dependence of relative resistivity on temperature for 2041, fired at 850 °C on Al_2O_3 and ZrO_2 substrates. (c) The dependence of relative resistivity on temperature for 3414-A, fired at 850 °C on Al_2O_3 and ZrO_2 substrates. (d) The dependence of relative resistivity on temperature for 8241, fired at 850 °C on Al_2O_3 and ZrO_2 substrates.

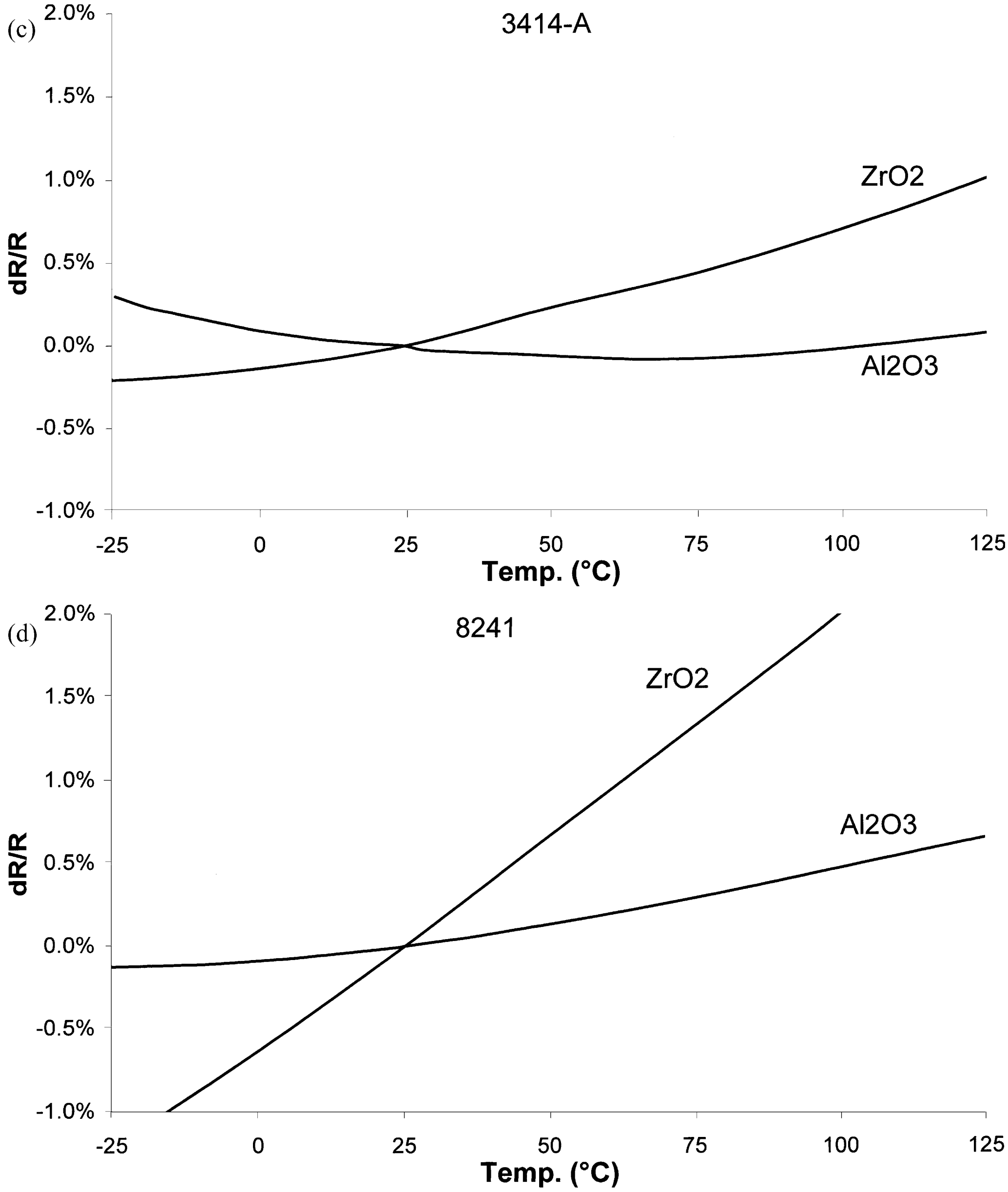

Fig. 7. (*continued*)

some 10 k ohm^2. resistors that were fired at 850 °C on alumina and zirconia substrates, are shown in Figs. 2a and b, and 3a and b for and 3414-A, respectively. The ceramic substrate is on the right. The microstructure of resistors consists of light grains of conductive phase imbedded in the grey glass phase. The glass phase is indicated by arrows.

The X-ray spectra of the resistors, that were fired on Al_2O_3 and ZrO_2 substrates are shown in Fig. 4a–d. The peaks of RuO_2 and the ruthenate phase are denoted "R" and "RU", respectively. The spectra are nearly the same, which confirms the compatibility of the tested 10 k ohm^2. resistors with the zirconia ceramics.

Sheet resistivities, cold (−25 to 25 °C) and hot (25 to 125 °C) TCRs, noise indices and gauge factors (GFs) of the resistors fired on the alumina and zirconia ceramics are presented in Table 3. The noise indices and GFs are also shown graphically in Figs. 5 and 6, respectively. The dependence of the relative resistivity vs. temperature is presented in Fig. 7. However, note that in Fig. 5 the noise indices are expressed in "uV/V" while in Table 3. they are given as "dB". These two units are related with an equation:

$$\text{noise (dB)} = 20 \times \log \text{noise (uV/V)}$$

The sheet resistivities and gauge factors of the resistors on the Al_2O_3 and ZrO_2 substrates are comparable. The GFs of 8241 resistors on alumina are around 15. This value is slightly higher than the value reported in the literature (GF around 13).[17] The noise indices are also comparable with the exception of the 3414-A that was fired on alumina which had a significantly higher noise of 2.75 uV/V. The noise indices of 2041 resistors have the lowest values. However, the TCRs of the resistors on the ZrO_2 are considerably higher. The hot TCR values are in all cases over 100×10^{-6}/K. The highest values, over 250×10^{-6}/K were measured for 8241. This is probably due to the higher thermal expansion coefficient of the tetragonal zirconia when compared with alumina (see Table 1).

4. Conclusions

The characteristics of some 10 k ohm^2. thick-film resistors that were fired on alumina and on tetragonal zirconia substrates were investigated with the aim of determining the compatibility of the resistor materials which were developed for firing on Al_2O_3, with ZrO_2 substrates. At the interface between the ZrO_2 and the resistor no interactions or evidence for new phases could be detected by SEM analysis. The X-ray spectra of the resistors fired on Al_2O_3 and ZrO_2 substrates are nearly the same. The sheet resistivities and noise indices (with the exception of the 3414-A resistors) of the resistors on Al_2O_3 and ZrO_2 are comparable. The high positive TCRs of the resistors on the ZrO_2 can be attributed to the higher thermal expansion coefficient of tetragonal zirconia. All the obtained results confirm the compatibility of the evaluated thick-film resistors with tetragonal zirconia ceramics. Therefore, the tested thick-film resistor materials could be made on tetragonal zirconia substrates if an allowance is made for the increased TCR.

Acknowledgements

The authors wish to thank Mr. Mitja Jerlah (HIPOT) for printing and firing the samples as well as for the TCR, noise and GF measurements, and Mrs. Jena Cilenšek (Jožef Stefan Institute) for the preparation of samples for SEM analysis. The work was carried out as a part of ''Development of zirconia based nanomaterials for applications using electrochemical and mechanical properties'' NATO Project SfP 974054. The financial support of the Ministry of Education, Science and Sport of the Republic of Slovenia is gratefully acknowledged.

References

1. Hoffman, K., *An Introduction to Measurements Using Strain Gauges*. Hottinger Baldwin Messtechnik GmbH, Darmstadt, 1989.
2. White, N. and Cranny, A., Design and fabrication of thick film sensors. *Hybrid Circuits*, 1987, **12**, 32–35.
3. White, N. M. and Turner, J. D., Thick film sensors: past, present and future. *Meas. Sci. Technol*., 1997, **8**(1), 1–20.
4. Prudenziati, M. and Morten, B., Piezoresistive properties of thick film resistors; an overview. *Hybrid Circuits*, 1986, **10**, 20–23, 37.
5. Hrovat, M., Belavič, D., Samardžija, Z. and Holc, J., A characterisation of thick film resistors for strain gauge applications. *J. Mater. Sci*., 2001, **36**, 2679–2689.
6. Satoh, S., Takatsuji, Y., Katoh, F. and Hirata, H. Thick film pressure sensor using zirconia diaphragm. In *Proc. 1991 Int. Symp. on Microelectronics ISHM-91*, Orlando, 1991, pp. 148–152.
7. Vest, R. W., Materials science of thick film technology. *Ceram. Bull*., 1986, **65**(4), 631–636.
8. Prudenziati, M., Morten, B. and Maseoro, A., Excess noise and refiring processes in thick film resistors. *J. Phys. D; Appl. Phys*., 1981, **14**(7), 1355–1362.
9. Yamaguchi, T. and Kato, S., Evaluation of commercial 96% alumina substrates and mechanism of paste-substrate interaction. *Ceram. Trans*., 1990, **15**, 575–582.
10. Morten, B., Masoero, A., Prudenziati, M. and Manfredini, T., Evolution of ruthenate-based thick film cermet resistors. *J. Phys. D: Appl. Phys*., 1994, **27**(10), 2227–2235.
11. Hrovat, M., Samardžija, Z., Holc, J. and Belavič, D., Microstructural, XRD and electrical characterisantion of some thick film resistors. *J. Mater. Sci.; Mat. Electron*., 2000, **11**(3), 199–208.
12. Hrovat, M., Belavič, D., Samardžija, Z. and Holc, J., A characterisation of thick film resistors for strain gauge applications. *J. Mater. Sci*., 2001, **36**(11), 2679–2689.
13. Chitale, S., Huang, C. and Stein, M., High gauge factor thick film resistors for strain gauges. *Hybrid Circuits Technol*., 1989, **6**(5), 15–18.
14. Hrovat, M., Belavič, D., Benčan, A. and Holc, J., Evaluating the compatibility of some thick-film resistors and tetragonal zirconia. *J. Mater. Sci. Lett*., 2001, **20**, 1605–1607.
15. Hrovat, M., Belavič, D., Holc, J. and Šoba, S., An evaluation of some commercial thick film resistors for strain gauges. *J. Mater. Sci. Lett*., 1994, **13**, 992–995.
16. Shah, J. S., Strain sensitivity of thick film resistors. *IEEE Trans. Components, Hybrids Manufact. Technol., CHMT-3*, 1980, **4**, 554–564.
17. Faecett, N. and Hill, M., The electrical response of thick-film resistore to hydrostatic pressure and uniaxial stress between 77 and 535 K. *Sensors and Actuators A, Physical*, 1999, **78**(2–3), 114–119.